

OBSERVATIONS OF CARBON AND OXYGEN ISOTOPIC HETEROGENEITY TOWARD PROTOSTARS RANGING IN MORPHOLOGY AND PARENT CLOUD. Rachel L. Smith^{1,2}, Klaus M. Pontoppidan³, Geoffrey A. Blake^{4,5}, Alexandra C. Lockwood⁴, ¹North Carolina Museum of Natural Sciences (rachel.smith@naturalsciences.org), ²Appalachian State University, Department of Physics and Astronomy, ³Space Telescope Science Institute, ⁴California Institute of Technology, Division of Geological and Planetary Sciences, ⁵Division of Chemistry and Chemical Engineering.

Introduction: High-resolution near-infrared (IR) observations of carbon monoxide (CO) gas enables precise derivation of C and O isotope ratios toward Solar-type protostars, and are powerful tools in furthering our understanding of early Solar System chemistry (e.g. [1,2]). These data have been used to investigate several isotopic peculiarities, including the $^{12}\text{C}/^{13}\text{C}$ Solar-ISM discrepancy [3-9], and the oxygen isotope anomaly found in meteorites [10]. Thus far, high-resolution observations have revealed significant heterogeneity in $^{12}\text{CO}/^{13}\text{CO}$ toward a set of low-mass protostars [11,12], and comparison of gas-phase $^{12}\text{CO}/^{13}\text{CO}$ ratios to CO ice abundance toward a set of low-mass protostars [11,12] has advanced considerations of protostellar ice-gas partitioning [11-14]. Further, observational signatures of mass-independent fractionation in oxygen isotopes toward a protostellar disk [2] have lent support for CO self-shielding on disk surfaces [15,16], and high-resolution observations of $^{12}\text{C}^{18}\text{O}$ and $^{12}\text{C}^{17}\text{O}$ toward low-mass protostars [11] have been used to support early Solar System supernova enrichment [17,18].

Toward refining our view of spatial isotopic variability for protostars dispersed in the same star-forming cloud, and to expand the CO survey comparing clouds, we present new results in Ophiuchus and an embedded binary system in Serpens. In addition, our new observations of massive protostars will hopefully shed light on phenomena in these complex regions which may affect other isotopic reservoirs (e.g. [19,20]).

Observations: Very high-resolution near-IR CO spectra toward local, low-mass protostars were obtained with the CRIRES spectrograph ($R \sim 95,000$) on the Very Large Telescope. Our new survey of massive protostars utilizes the NIRSPEC spectrograph ($R \sim 25,000$) on the Keck Telescope. Figure 1 (top) shows a portion of the fundamental bands ($v = 1 - 0$) for the embedded binary protostar, EC 90 (0,1) in Serpens, observed with CRIRES; and (bottom) a portion of the NIRSPEC spectrum for the massive protostar AFGL 2136 in the Juggler Nebula. Overtone ($v = 2 - 0$) spectra (not shown) were used for observing optically thin $^{12}\text{C}^{16}\text{O}$ lines. Total column densities for each isotopologue were precisely determined using the CRIRES spectral lines, and the carbon and oxygen isotope ratios thereby derived (this method is described in detail in [2,12]).

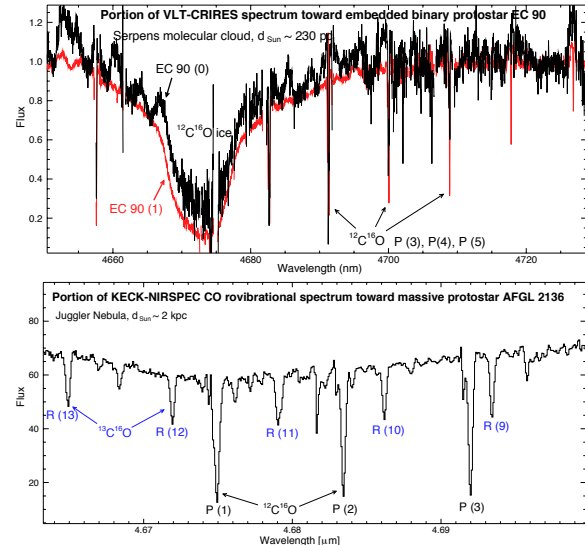


Figure 1: (Top): Portion of the near-IR VLT-CRIRES CO fundamental rovibrational bands toward the low-mass binary, EC 90 (Serpens); (Bottom): Portion of the Near-IR Keck-NIRSPEC CO fundamental band toward the massive protostar, AFGL 2136 (Juggler Nebula). Representative CO isotopologue lines and ice features are marked.

Results and discussion: Significant range is found in robust $^{12}\text{CO}/^{13}\text{CO}$ ($\sim 85 - 165$), notably between the 6 Ophiuchus targets (Figure 2). The $^{12}\text{CO}/^{13}\text{CO}$ for each of the components of the binaries DoAr24E(0,1) [98 ± 1 and 102 ± 3] and EC90(0,1) [130 ± 4 and 140 ± 16] are within error to each other. The low-temperature ratio for VV CrA(N) [127 ± 2], not shown in Figure 2), is nearly identical to that of its cold-gas companion, VV CrA(S) [127 ± 1]. Our results suggest that low-mass binaries (gas within ~ 200 to 300 AU) may be isotopically more homogeneous than single protostars dispersed across the same cloud/cloud complex, and between protostars in different clouds. Figure 3 compares the gas-phase $^{12}\text{CO}/^{13}\text{CO}$ and the CO ice fraction. Our new data add to the group of targets where only cold gas is present, resulting in cold-temperature isotope ratios that are likely more robust than the cold-temperature ratios derived where a warm temperature regime is also present. The suggested trend in the cold-only regimes suggests that ice-gas interaction may be contributing to the $^{12}\text{CO}/^{13}\text{CO}$ heterogeneity. Figure 4 compares oxygen data for the latest CRIRES sample. A mass-independent signature is seen in disks VV CrA [2] and HL Tau, and disk/envelope, WL 6 [12].

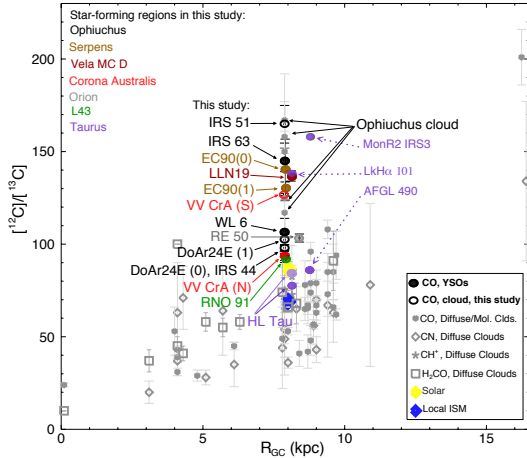


Figure 2: Compilation of $[^{12}\text{C}]/[^{13}\text{C}]$ vs. R_{GC} (kpc), and data from this study, some of which are from [2,11,12]. The CRIRES $[^{12}\text{CO}]/[^{13}\text{CO}]$ from this study are shown at left (labels and filled dots). The local ISM (~ 68 [8]) and Solar ~ 87 [6] are shown. Color-coded molecular clouds associated with each protostar is shown at top, left. Infrared data for HL Tau (lower value [1]) and 3 embedded protostars [21] are marked (purple; right-side labels). The black arrows indicate $[^{12}\text{CO}]/[^{13}\text{CO}]$ in diffuse Ophiuchus gas [22,23].

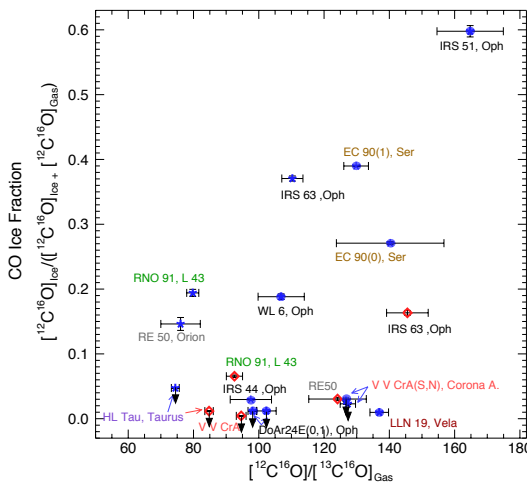


Figure 3: Comparison of CO ice fraction vs. the $[^{12}\text{C}]/[^{13}\text{C}]_{\text{Gas}}$ for the CRIRES sample. Protostars and parent clouds are labeled. Blue stars indicate cold-gas isotope ratios from regimes where warm gas (red diamonds) was also observed. Blue ovals indicate objects where only cold gas was observed. Total CO ice values were derived from pure CO ice optical depths [24,25]. Some data are from [11,12]. Downward arrows are $3 - \sigma$ upper limits on CO ice.

Results for EC 90,1 (Serpens) and IRS 44 (Ophiuchus) cannot be differentiated from mass-dependence.

Conclusions: Our CO survey now totals 15 local protostellar site-lines, representing 7 star-forming clouds and 3 binary systems. Significant $[^{12}\text{CO}]/[^{13}\text{CO}]$ heterogeneity is observed in embedded protostars in different clouds, as well as for those

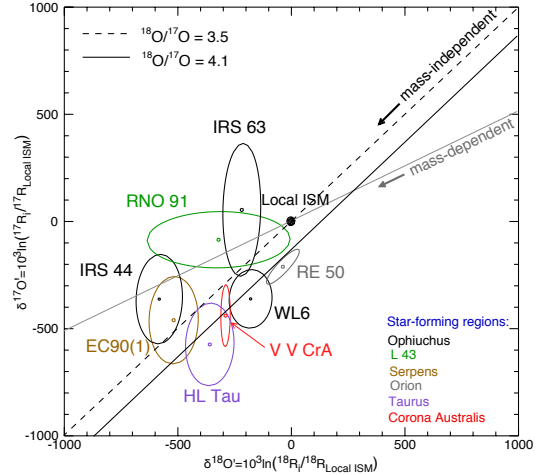


Figure 4: Comparison of the ISM and CRIRES targets (labeled) where 3 oxygen isotopes were observed. Represented molecular clouds are noted and color-coded at bottom right. Ellipses are $1 - \sigma$. A portion of these data are from [2,12].

dispersed within the same cloud, results which could be tracers of varying chemical paths for protostellar cores separated in the parent cloud. The set of robust cold-gas data adds support for ice-gas interaction influencing gas-phase $[^{12}\text{CO}]/[^{13}\text{CO}]$. Heterogeneity in oxygen isotopes for the Ophiuchus targets may also correlate with protostellar evolutionary stage. Our results suggest potential carbon isotopic homogeneity within a few hundred AU for low-mass protostars. Ongoing analyses include massive protostars and additional isotopic reservoirs, which will hopefully continue to inform our understanding of early protostellar phenomena.

References: [1] Brittain S.D. et al. (2005) *ApJ* 626, 283-291.[2] Smith R.L. et al. (2009) *ApJ* 701, 163-175.[3] Coplen T.B. et al. (2002) *Pure Appl. Chem.* 74, 1987-2017.[4] Clayton D.D. and Nittler L.R. (2004) *ARA* 42, 39-78.[5] Wilson T.L. (1999) *Rep. Prog. Phys.* 62, 143-185.[6] Scott P.C. et al. (2006) *A&A.* 456, 675-688.[7] Langer W.D. and Penzias A.A. (1993) *ApJ* 408, 539-547.[8] Milam S.N. et al. (2005) *ApJ* 634, 1126-1132.[9] Bensch et al. (2001) *ApJ* 562, L185-L188.[10] Clayton R.N. et al. (1973) *Science* 182, 458-488.[11] Smith R.L. et al. (2011) *42nd LPI*, 1608, 1281.[12] Smith R.L. et al. (2013), *ApJ*, in review.[13] Pontoppidan K.M. (2006) *A&A* 453, L47.[14] Young E.D. and Schauble E.A. *42nd LPI*, 1608, 1323. [15] Lyons J.R. and Young E.D. (2005) *Nature* 435, 7040, 317- 320. [16] Young, E.D. et al. (2008) *RiMG*, 68, 187.[17] Gounelle M. and Meibom A. (2007) *ApJ* 664, L123-L126.[18] Young E.D. et al. (2011) *ApJ*, 729, 43.[19] Boogert A.C.A. et al. (2000) *A&A* 353, 349-362.[20] Boogert A.C.A. et al. (2002) *ApJ* 577, 271-280. [21] Goto M. et al. (2003) *ApJ* 598, 1038-1047. [22] Federman S.R. et al. (2003) *ApJ* 591, 989-999.[23] Lambert D.L. et al. (1994) *ApJ* 420, 756-771.[24] Pontoppidan K.M. et al. (2003) *A&A* 408, 981-1007.[25] Thi W.-F. et al. (2006) *A&A* 449, 251-265.